JPET Fast Forward. Published on June 30, 2008 as DOI: 10.1124/jpet.108.139733

1-[1-hexyl-6-(methyloxy)-1*H*-indazol-3-yl]-2-methyl-1-propanone (HMIMP), a Potent and Highly Selective Small Molecule Blocker of the Large-Conductance Voltage-gated and Calcium-dependent K^+ Channel

Haoyu Zeng, Earl Gordon, Zuojun Lin, Irina M. Lozinskaya, Robert N. Willette, and Xiaoping Xu

Metabolic Pathway Center of Excellence in Drug Discovery, GlaxoSmithKline, King of Prussia, PA 19406, USA (H.Z., E.G., Z.L., I.M.L., R.N.W. and X.X.)

a) Running Title: Small molecule BK channel blocker

b) Correspondence Author: Xiaoping Xu, GlaxoSmithKline, 709 Swedeland Road, UW2511, PO Box 1539, King of Prussia, PA 19406, USA

Telephone: (610) 270-6858

Fax: (610) 270-6206

E-mail: Xiaoping.2.Xu@gsk.com

c) Number of Text pages: 26

Number of Tables: 0

Number of Figures: 8

Number of References: 29

Number of words in the Abstract: 250

Number of words in the Introduction: 409

Number of words in the Discussion: 689

d) Abbreviations: BK channel, large-conductance voltage-gated and calcium-dependent K^+ channel; CHO, Chinese hamster ovary; HMIMP, 1-[1-hexyl-6-(methyloxy)-1*H*-indazol-3-yl]-2-methyl-1-propanone; hERG, human ether-a-go-go-related gene; I-V, current-voltage relationship; I_{to}, transient outward K^+ current; K_V channel, voltage-gated K^+ channel

e) Recommended section: Cellular and Molecular

Abstract

The large-conductance voltage-gated and calcium-dependent K^+ (BK) channels are widely distributed and play important physiological roles. Commonly used BK channel inhibitors are peptide toxins isolated from scorpion venoms. A high-affinity, non-peptide, synthesized BK channel blocker with selectivity against other ion channels has not been reported. We prepared several compounds from a published patent application (Doherty, et al., 2004) and identified 1-[1-hexyl-6-(methyloxy)-1*H*-indazol-3-yl]-2-methyl-1-propanone (HMIMP) as a potent and selective BK channel blocker. The patch-clamp technique was used for characterizing the activity of HMIMP on recombinant human BK channels (α subunit, α+β1 and α+β4 subunits). HMIMP blocked all these channels with an IC_{50} of ~2 nM. The inhibitory effect of HMIMP was not voltage-dependent, nor did it require opening of BK channels. HMIMP also potently blocked BK channels in freshly isolated detrusor smooth muscle cells and vagal neurons. HMIMP (10 nM) reduced the open probability significantly without affecting single BK channel current in inside-out patches. HMIMP did not change the time constant of open states but increased the time constants of the closed states. More importantly, HMIMP was highly selective for the BK channel. HMIMP had no effect on human $Na_V1.5$ (1 μM), $Ca_V3.2$, L-type Ca^{2+}, hERG, KCNQ1+minK, transient outward K^+ or voltage-dependent K^+ channels (100 nM). HMIMP did not change the action potentials of ventricular myocytes, confirming its lack of effect on cardiac ion channels. In summary, HMIMP is a highly potent and selective BK channel blocker which can serve as an important tool in the pharmacological study of the BK channel.

Introduction

The large-conductance voltage-gated and calcium-dependent K^+ (BK) channels are widely distributed in smooth muscle, neuron and many other tissues, and plays important roles in many physiological events (for a recent review, see (Ghatta, et al., 2006)). BK channel contains four α subunits that form the channel pore (Atkinson, et al., 1991), and different auxiliary β subunits that modulate the channel properties (Garcia-Calvo, et al., 1994; Knaus, et al., 1994a). Four mammalian β subunits have been identified: the β1 subunit increases the Ca^{2+}/voltage sensitivity of BK channel and slows its kinetics (McManus, et al., 1995; Brenner, et al., 2000b); β2 (Wallner, et al., 1999; Xia, et al., 2003) and β3 (Xia, et al., 2000; Brenner, et al., 2000a) subunits cause BK channel inactivation; and β4 subunit alters channel kinetics (Brenner, et al., 2000a; Brenner, et al., 2005).

Several widely used BK channel inhibitors, such as iberiotoxin (Galvez, et al., 1990), charybdotoxin (Miller, et al., 1985) and slotoxin (Garcia-Valdes, et al., 2001), are peptide toxins isolated from various scorpion venoms. Recently, two more BK channel blockers, BmBKTx1 (Xu, et al., 2004) and BmP09 (Yao, et al., 2005), were identified in scorpion toxins. Peptide toxins with different pharmacological properties are widely used to study BK channels. However, β subunits modulate the interaction between these peptide toxins and the α subunit, and the neuronal BK channels formed by α+β4 subunits are resistant to iberiotoxin, charybdotoxin and slotoxin (Meera, et al., 2000; Garcia-Valdes, et al., 2001; Lippiat, et al., 2003). Non-peptide, alkaloid BK channel blockers, such as paxilline, penitrem A, verruculogen and tetrandrine, are also useful

JPET Fast Forward. Published on June 30, 2008 as DOI: 10.1124/jpet.108.139733
This article has not been copyedited and formatted. The final version may differ from this version.

pharmacological tools for examining BK channels (Knaus, et al., 1994b; Wu, et al., 2000; Tammaro, et al., 2004). Paxilline blocks BK channels in a Ca^{2+}-dependent manner, and it potently inhibits BK channels with low free Ca^{2+}-concentrations (Sanchez and McManus, 1996). Recently, a small molecule A-272651 has been reported to inhibit BK channel with an IC_{50} of ~5 μM which is 1000 fold less potent than the peptide BK channel blockers (Shieh, et al., 2007). High-affinity, synthesized small molecule BK channel blockers with good ion channel selectivity remain to be identified.

We prepared several compounds from a published patent application (Doherty, et al., 2004) and identified a highly potent BK channel blocker, 1-[1-hexyl-6-(methyloxy)-1*H*-indazol-3-yl]-2-methyl-1-propanone (HMIMP), with single digit nanomolar potency and good ion channel selectivity (>50-fold). HMIMP, as a highly potent and selective small molecule BK channel blocker, is a very useful tool for examining the pharmacology of BK channels.

JPET Fast Forward. Published on June 30, 2008 as DOI: 10.1124/jpet.108.139733
This article has not been copyedited and formatted. The final version may differ from this version.

Methods

Cell culture. Chinese hamster ovary (CHO) cells were stably transfected to express different recombinant channels, including the human BK α subunit, BK α+β_1 subunits, BK α+β_4 subunits, hERG or human KCNQ1+minK. HEK 293 cells were used to stably express the human $Na_V1.5$ α subunit or $Ca_V3.2$ (α_{1H}) channels. All cell lines were generated at GlaxoSmithKline (King of Prussia, PA) and maintained at 37˚C with 5% CO_2 in T-75 flasks or 6-well culture dishes in appropriate media.

Cell isolation. The studies were carried out in accordance with the Guide for the Care and Use of Laboratory Animals as adopted and promulgated by the U.S. National Institutes of Health and approved by the GlaxoSmithKline Animal Care and Use Committee. Single myocytes were isolated from the right ventricle of adult male New Zealand White rabbits using enzyme digestion described previously (Rials, et al., 1997). Myocytes were also isolated from the right ventricle of adult male guinea pigs using the same isolation protocol, except that the enzyme solution perfusion was abbreviated to 5 min. Only rod-shaped, quiescent cells with obvious striations were used for the experiments. The procedure of detrusor smooth muscle cell isolation has been described in detail previously (Ghatta, et al., 2007). To isolated single vagal neurons, mice of either sex were euthanized by carbon dioxide asphyxiation. Nodose jugular complex was rapidly removed bilaterally. They were incubated in enzyme solution which is composed of collagenase type 1 (2 mg/mL) (Sigma, St. Louis) and dispase II (2 mg/mL) (Roche, Indianapolis) in Ca^{2+} - and Mg^{2+}- free Hank`s balanced salt solution for 1 hr at room temperature. Neurons were dissociated by trituration, washed by centrifugation (2 times at 1000g for 5 minutes), suspended in L-15 medium (Invitrogen)

containing 10% fetal bovine serum, and transferred on to poly-l-lysine coated coverslips (BD Biosciences, Bedford). Neurons adhered to coverslips and were maintained for 15 hrs prior to recording. Neurons were used up to 24 hrs after isolation and there was no neurite outgrowth observed. To isolate arterial smooth muscle cells, adult male guinea pigs were sacrificed by sodium pentobarbital overdose. Small mesenteric arteries were removed from the animal. Fat and connective tissue were removed in a cold, nominal Ca^{2+}-free solution containing (in mM) 137 NaCl, 5 KH_2PO_4, 1 $MgSO_4$, 10 glucose, 5 HEPES, 8 taurine and 1 mg/mL bovine serum albumin; pH 7.4. The vessels were cut into tiny pieces and incubated in nominally Ca^{2+}-free solution on ice for about 20 min. The tissue pieces were then transferred to an enzyme solution made by adding 50 μM $CaCl_2$, 1.5 mg/mL collagenase type II (Worthington Biochemical Corporation), 1 mg/mL protease XXIV (Sigma), and 0.25 mg/mL trypsin inhibitor (Sigma) to nominally Ca^{2+}-free solution. Tissues in enzyme were stored on ice for 2 to 3 hours and then incubated in a 37°C water bath and bubbled with 100% O_2. The enzyme solution was checked periodically for single smooth muscle cells. Cells were harvested in the supernatant by centrifugation. The digestion and collection procedure was repeated twice. Isolated cells were stored at 4°C in a solution composed of (in mM) 80 potassium glutamate, 20 K_2HPO_4, 20 KCl, 5 $MgCl_2$, 0.5 K_2EGTA, 2 Na_2ATP, 5 Na-pyruvate, 5 creatine, 20 taurine, 10 glycine, 10 glucose, and 5 HEPES. Cells were used for experiments within 6 hours of isolation.

Current recording. All currents were recorded at room temperature (~23^{o}C) (with the exception of $Na_V1.5$ current measured at 13±0.4^{o}C) using an Axopatch 200B amplifier and Digidata 1322A digitizer (Molecular Devices, Union City, CA). Cells were placed in

a small chamber (volume=0.7 mL) and continuously perfused with an external solution (3-4 mL/min). Electrodes were pulled from thin wall glass (WPI, Sarasota, FL) using a P-97 horizontal puller (Shutter, Novato, CA) and fire polished with MF-830 microforge (Narishige, Long Island, NY). Electrode resistance was with 2-3 MΩ for whole-cell and 8-15 MΩ for inside-out patch recordings. Currents were elicited by different voltage protocols (described in text and figure legends) and acquired with pCLAMP 8 software (Molecular Devices). Single channel currents were filtered at 2 kHz and digitized at 25 kHz.

Action potential recording. Action potentials were recorded from single guinea pig or rabbit ventricular myocytes at 36±0.3^{o}C using the microelectrode technique at a stimulus frequency of 1 Hz. The microelectrode was made using a KOPF pipette puller (DAVID KOPF Instruments, Tujunga, CA) and had a resistance of 25-40 MΩ when filled with 3 M KCl. Action potentials of single guinea pig detrusor smooth muscle cells were recorded at 35±0.4^{o}C using the whole-cell current-clamp (1.6-ms super-threshold depolarizing current pulses given at 0.5 Hz).

Solutions. Unless otherwise stated, bath solution for current and action potential recording contained (in mM) 140 NaCl, 4 KCl, 1 $MgCl_2$, 2 $CaCl_2$, 10 Glucose, and 10 HEPES, pH=7.4. Bath solution for $Na_V1.5$ current (in mM): 14 NaCl, 126 NMDG-Cl, 4 KCl, 1 $MgCl_2$, 2 $CaCl_2$, 10 Glucose, and 10 HEPES, pH=7.4. Bath solution for L-type Ca^{2+} current (in mM): 135 NaCl, 5 CsCl, 1 $MgCl_2$, 2 $CaCl_2$, 10 Glucose, 10 HEPES; pH = 7.4. Bath solution for transient outward K^+ current (in mM): 140 NMDG-Cl, 5 KCl, 1 $MgCl_2$, 1 $CaCl_2$, 10 Glucose, and 10 HEPES, 0.3 $CdCl_2$, 0.1 $BaCl_2$. Pipette solution which contained (in mM) 140 KCl, 5 EGTA, 1 $MgCl_2$, 5 MgATP, 0.2 $CaCl_2$ and 5

HEPES, pH = 7.2 (6.5 nM free Ca^{2+}) was used for recording detrusor action potentials and all the currents unless otherwise stated. A similar pipette solution containing 1.4 mM $CaCl_2$ was used for neuronal BK current recording (61 nM free Ca^{2+}). Pipette solution for L-type Ca^{2+} current (in mM): 151 CsOH, 10 L-aspartic acid, 20 taurine, 20 tetraethylammonium chloride, 5 glucose, 10 EGTA, adjust pH to 7.5 with H_3PO_4. MgATP (5 mM) and guanosine triphosphate (0.4 mM sodium salt) were added to the pipette solution before use and the final pH was 7.3. Internal solution for recording $Na_V1.5$, $Ca_V3.2$, hERG and KCNQ1+minK current (in mM): 119 K-gluconate, 15 KCl, 5 EGTA, 5 K_2ATP, 3.2 $MgCl_2$, 5 HEPES, pH=7.2. Single channel bath solution contained (in mM) 140 KCl, 1 $MgCl_2$, 2 $CaCl_2$ 5 EGTA, 5 HEPES, pH=7.2 (100 nM free Ca^{2+}), and pipette solution contained (in mM) 150 KCl, 1 $MgCl_2$, 1 $CaCl_2$, 5 HEPES, pH 7.2. The free Ca^{2+} concentrations of solutions were calculated using Webmaxc (http://www.stanford.edu/~cpatton/webmaxcS.htm).

Chemicals. 1-[1-hexyl-6-(methyloxy)-1*H*-indazol-3-yl]-2-methyl-1-propanone (HMIMP, see Fig. 8 for structure) was synthesized at GlaxoSmithKline (King of Prussia, PA). HMIMP was dissolved in dimethyl sulfoxide to make 1 mM stock solution and stored at -20^{o}C. The drug stock solution was diluted in external solutions to desired concentrations and used within 3 hrs. The effects of HMIMP were determined when drug response reached steady-state after 3-5 min of perfusion with the compound.

Data analysis. Whole-cell currents were analyzed using pClamp 8 (Molecular Devices, Union City, CA). Single channel currents were analyzed with Fetchan and PStat bundles in the pClamp 8 software. Events list were created in Fetchan using a 50 %-threshold crossing approach to determine open events, no minimum-duration level was

imposed when detecting transitions between closed and open states. The single channel amplitudes were obtained by forming amplitude histograms of selected regions of recordings that had clear single open and closed current levels. Gaussian distributions were fitted to the amplitude histograms to determine the unitary current. The dwell time distributions of open and closed current levels were constructed from patches containing only one active channel. Open dwell time distribution histograms were fitted with a single exponential, and closed dwell time distribution histograms were fitted with a double exponential: $F(t)= A_{fast}*\exp(-t/tau_{fast}) + A_{slow}*\exp(-t/tau_{slow})$ (1), where A_{fast} and A_{slow} are the amplitude terms of the fast (tau_{fast}) and slow (tau_{slow}) time constants, respectively. A Simplex algorithm was used to perform non-linear least-squared fits. Data were presented as mean±S.E. (n). Statistical significance ($P<0.05$) was determined using one-way ANOVA, one-population *t*-test or paired *t*-test.

Results

We first studied the effects of HMIMP on human BK α subunit stably expressed in CHO cells. Whole-cell current were elicited by 200-ms depolarizing steps to different voltages (+30 to +140 mV in 10-mV increments) from a holding potential of 0 mV (inset of Fig. 1A), inter-pulse interval was 2-s. The characteristic, fast-activating BK currents were recorded under control conditions and 30 nM HMIMP almost completely abolished the currents (Fig. 1A). We next examined the concentration-dependent inhibition of human BK α subunit by HMIMP. BK current inhibition (%) was calculated using current amplitudes after drug effect reached steady-state against those prior to HMIMP treatment at various voltages. The IC_{50} value of each concentration-response curve was obtained by fitting the curve with the logistic equation. HMIMP blocked human BK α subunit with IC_{50} of 1.7±0.6, 2.1±0.8, 2.3±0.8, 2.9±0.9 nM (n=5) at +80, +100, +120, and +140 mV, respectively (Fig. 1B). The differences in IC_{50} values were not statistically significant. We then examined whether the effect of HMIMP was use-dependent. BK current was recorded using the voltage-clamp protocol (as the inset of Fig. 1A but in the voltage range +70 to +110 mV) in control solution (Fig. 1C, left). After perfusing the cell with 3 nM HMIMP for 5 min without stimulation, BK currents were recorded twelve times using the same voltage-clamp protocol, the first and last recordings in drug were compared (Fig. 1C, middle and right). There was no additional block with the opening of BK channels.

Different β subunits of the BK channel conveyed differential sensitivity to Iberiotoxin. Iberiotoxin can potently inhibit BK α, α+$β_1$ and α+$β_3$, but not α+$β_4$ (Meera, et al., 2000;

JPET Fast Forward. Published on June 30, 2008 as DOI: 10.1124/jpet.108.139733
This article has not been copyedited and formatted. The final version may differ from this version.

Lippiat, et al., 2003). Therefore, we examined whether different β subunits would modify the blocking effect of HMIMP on BK α subunit. CHO cells stably expressing human BK $\alpha+\beta_1$ or $\alpha+\beta_4$ subunits were used. Whole-cell currents were elicited with the same protocol, and data were processed in the same way as described in Fig. 1. In the presence of β_1 (the smooth muscle isoform) or β_4 subunits (the neuronal isoform), BK channel activation was much slower compared with channels composed of the α subunit alone (comparing insets of Fig. 2 to Fig. 1A), as described elsewhere (Lippiat, et al., 2003). The concentration-responses measured at +100 mV showed that HMIMP inhibited BK channels with an IC_{50} of 2.1±0.6 nM for α+β1 and 1.5±0.4 nM for α+β4 (Fig. 2A and B). The IC_{50} values were not significantly different from each other or from that of channels composed of the α subunit alone. HMIMP (30 nM) also blocked the BK current in freshly isolated rabbit detrusor smooth muscle cells (Fig. 2C) and mouse vagal neurons (Fig. 2D), suggesting that HMIMP can act on native BK channels of different species.

Single channel current was recorded in inside-out patches of CHO cells stably expressing the human BK α subunit. HMIMP (10 nM) reduced single channel open probability from 0.120±0.051 to 0.014±0.004, an average 81±4% reduction (n=7), but had no significant effect on single channel current, 18.1±0.8 pA in control and 18.0±0.8 pA (n=7) in drug recorded at +80 mV (Fig. 3A-C). The extent of BK α channel block by 10 nM HMIMP in inside-out patches was comparable to that observed in the whole-cell condition. HMIMP did not affect the time constant of open states (Fig. 3D), 7.8±1.5 ms in control and 9.6±1.6 ms (n=7) in drug. HMIMP increased the fast and slow time

constants of the closed state from 21.3±3 ms and 194.7±39.5 ms to 41.9.0±7.1 ms and 485.3±70.5 ms (n=7), respectively, after drug treatment ($P<0.05$) (Fig. 3E). However, the ratio of the amplitude for the fast component to the sum of the amplitude of both components [$A_{fast}/(A_{fast}+A_{slow})$] was unchanged, 0.71±0.07 versus 0.83±0.04 (n=7) for control and in the presence of 10 nM HMIMP, respectively.

The selectivity of HMIMP against other ion channels expressed in the cardiovascular system was examined. Na^+ currents were elicited from HEK 293 cells stably expressing human $Na_V1.5$ channels by 30-ms depolarizing steps to different voltages (-60 to +30 mV in 10-mV increments) from a holding potential of -90 mV (inset of Fig. 4A), inter-pulse interval was 5-s. Na^+ currents were recorded at low temperature (13^{o}C) and in a reduced extracellular Na^+ concentration to ensure good voltage-clamp. Peak current amplitudes at various voltages were normalized to the maximal peak current amplitude of the cell prior to HMIMP treatment to obtain normalized current-voltage relationship (I-V) curve. HMIMP at 1 μM had no significant effect on the I-V curve of $Na_V1.5$ channels (Fig. 4A). T-type Ca^{2+} current was recorded from HEK293 cells expressing human $Ca_V3.2$ channels using the same voltage-clamp protocol as used for Na^+ current except for longer depolarizing steps (160-ms). HMIMP (100 nM) did not affect T-type Ca^{2+} current (Fig. 4B). L-type Ca^{2+} current in guinea pig ventricular myocytes were elicited by 180-ms depolarizing voltage steps to different voltages (-30 to +50 mV in 10-mV increments) from a holding potential of -40 mV (inset of Fig. 4C) in the presence or absence of 100 nM HMIMP (Fig. 4C). Inter-pulse interval was 5-s. Currents were normalized to the maximal current amplitude of the cell before application of HMIMP to

generate a normalized I-V curve (Fig. 4C). The L-type Ca^{2+} currents were not affected by 100 nM HMIMP.

The effect of HMIMP on hERG channels was investigated using the same protocols as described previously (Zeng, et al., 2006). Briefly, hERG currents in CHO cells were induced before and after 100 nM HMIMP application by 2-s depolarizing steps to different voltages (-70 to +60 mV in 10-mV increments) from a holding potential of -80 mV, followed by a 2-s hyperpolarizing step to -50 mV to measure tail currents (Fig. 5A). Inter-pulse interval was 10-s. To obtain normalized I-V curves, step current amplitudes measured as the mean current of the last 100-ms at various voltages were normalized to the maximal step current amplitude of the cell prior to HMIMP treatment. The bell-shape I-V curves revealed that HMIMP (100 nM) inhibited the hERG step currents only at +40 mV or above (Fig. 5B). However, 100 nM HMIMP had no effect on the voltage-dependent activation of hERG channels that were measured from the normalized peak tail currents (Fig. 5C).

Effects on KCNQ1+minK channels, which underlie the slowly activating delayed rectifier K^+ current in cardiac tissue, were evaluated. Current from CHO cells stably expressing human KCNQ1+minK were excited by 2.8-s depolarizing voltage steps to different voltages (-30 to +60 mV in 10-mV increments) from a holding potential of -90 mV, followed by a 1-s hyperpolarizing step to -50 mV (inset of Fig. 6A). The inter-pulse interval was 6-s. To generate normalized I-V curves, step current amplitudes at various voltages were normalized to the maximal step current amplitude of the cell prior to

HMIMP application. The result showed that HMIMP had no effect on the KCQN1+minK current at 100 nM (Fig. 6A). Similarly, the transient outward K^+ current (I_{to}) of rabbit ventricular myocytes was examined with a pulse protocol (Fig. 6B, inset) with or without 100 nM HMIMP. I_{to} current was induced by 160-ms pulses to different voltages (-10 to +40 mV in 10-mV increments) from a holding potential of -80 mV. Inter-pulse interval was 5-s. Peak currents were normalized to the maximal current amplitude prior to HMIMP application to evaluate the effect of HMIMP on I_{to}. The result clearly demonstrated that 100 nM HMIMP did not affect I_{to} current (Fig. 6B). Besides cardiac ion channels, we also examined whether HMIMP had any effect on the voltage-gated K^+ (K_V) channel in vascular smooth muscle cells. K_V currents were excited by 200-ms depolarizing voltage steps to different voltages (-40 to +40 mV in 10-mV increments) from a holding potential of -80 mV (inset of Fig. 6C) with or without 100 nM HMIMP. Inter-pulse interval was 5-s. Currents were normalized to the maximal current amplitude of the cell prior to HMIMP application to generate normalized I-V curve (Fig. 6C), showing no effect of HMIMP on K_V current.

Finally, we examined the overall effect of 100 nM HMIMP on cardiac ion channels by measuring the action potential of ventricular myocytes freshly isolated from guinea pig or rabbit heart. Action potentials were recorded with microelectrodes as described previously (Rials, et al., 1997). The action potential shape and duration were almost identical prior to or after application of 100 nM HMIMP in both guinea pig and rabbit ventricular myocytes (Fig. 7, top and middle panels). On the contrary, HMIMP (30 nM) dramatically prolonged the action potential and reduced after hyperpolarization of a

detrusor smooth muscle cell (Fig. 7, bottom panel) as expected, since BK channels play a critical role in the repolarization of the action potential of detrusor (Heppner, et al., 1997).

Discussion

Here, we reported a highly potent and selective, synthesized small molecule BK channel blocker HMIMP. It blocked recombinant human BK channels with an IC_{50} of ~2 nM, and the blocking potency was not affected by the membrane potential or co-expression of different BK β subunits. HMIMP also blocked native BK channels in smooth muscle cells and in vagal neurons which are mostly comprised of α+β1 subunits and α+β4 subunits, respectively.

As a widely distributed ion channel, the BK channels contribute to cellular functions in many tissues and is involved in certain human diseases (Ghatta, et al., 2006). Most widely used BK channel blockers are peptide toxins. HMIMP is a small molecule that has BK blocking potency greater than or equal to the “gold standard”, iberiotoxin. While both iberiotoxin and HMIMP have no effect on single BK channel current amplitude, they are distinct in many aspects. First, iberiotoxin blocks BK channels only from the extracellular side of the membrane, whereas HMIMP blocked BK channels from either side. Second, iberiotoxin produces long non-conducting silent periods, without affecting the gating kinetics of BK channels (Giangiacomo, et al., 1992), whereas HMIMP decreased the BK α channel open probability primarily by increasing the duration of channel closure, stabilizing the channel in the closed state. Third, BK channel accessory β1 subunit attenuates the potency of iberiotoxin tenfold (Lippiat, et al., 2003) and β4 renders the channel insensitive to iberiotoxin (Meera, et al., 2000), whereas neither β1 nor β4 affected the potency of HMIMP. Besides iberiotoxin, BK α+β4 channels are also resistant to charybdotoxin (Meera, et al., 2000) and slotoxin (Garcia-

Valdes, et al., 2001). Our results indicate that HMIMP is the most potent known BK α+β4 channel blocker and will have particular value for studying the functions of neuronal BK channels which contain the β4 subunit.

The lack of impact of β subunits on HMIMP blocking effect on BK channels implies that HMIMP may directly bind to the BK α subunit and the binding site is not interrupted by the association of β subunits. In addition, HMIMP blocked BK channel in a non-use dependent manner, which indicated that it was not an open channel blocker. Therefore, it is likely that HMIMP binds to the BK α subunit and blocks the channel allosterically, rather than directly occupying the channel pore.

Besides peptide BK channel blockers, alkaloids such as paxilline and tetrandrine also inhibit BK channels with an IC_{50} of 1.9 nM for BK α subunit and 5 μM for BK channels of an endothelial cell line (Sanchez and McManus, 1996; Wu, et al., 2000). However, Paxilline potently inhibits BK channel only at low free Ca^{2+}-concentrations (Sanchez and McManus, 1996). Tetrandrine also blocks voltage-dependent Ca^{2+} channels (Wang and Lemos, 1995). The only other known small molecule BK channel blocker, A-272651, has an IC_{50} of ~5 μM (Shieh, et al., 2007), 2500 times less potent than HMIMP.

Although with comparable IC_{50} values, there seems no obvious similarity between the two-dimensional structures of HMIMP and Paxilline (Fig. 8). As far as commonalities go, both structures have carbonyls as well as 5, 6 ring systems (indazole/indole) and ether oxygens, but the spatial relationships between these two types of moieties are

completely different when comparing HMIMP and Paxilline. We cannot exclude the possibility of the existence of three-dimensional correspondences between these two molecules, but it's very difficult to justify without knowing whether they bind to the same location in the BK channel and the key structural domains of each molecule.

In addition to being highly potent, HMIMP was also a very specific BK channel blocker. At ≥ 50 times the IC_{50} value for BK channel inhibition, HMIMP had no effect on various cardiovascular ion channels including $Na_V1.5$, $Ca_V3.2$, L-type Ca^{2+}, KCNQ1+minK, transient outward K^+ and K_V channels. Although HMIMP slightly reduced hERG step current, the effect occurred only at membrane potentials ≥ +40 mV which is non-physiological for cardiac myocytes. The lack of effects of HMIMP on action potentials of ventricular myocytes substantiated its specificity.

In summary, HMIMP is a potent and highly selective BK channel blocker which can serve as a useful tool in the study of the BK channel function.

Acknowledgments

The authors would like to thank Drs. Joseph Marino, Dennis Lee, and Steve Zhao at the Chemistry Department of Metabolic Pathway Center of Excellence in Drug Discovery for the synthesis of HMIMP and Dr. Srinivas Ghatta at the Biology Department of Respiratory & Inflammation Center of Excellence in Drug Discovery for isolation of neurons.

References

Atkinson NS, Robertson GA and Ganetzky B (1991) A component of calcium-activated potassium channels encoded by the Drosophila slo locus. *Science* **253**:551-555.

Brenner R, Chen QH, Vilaythong A, Toney GM, Noebels JL and Aldrich RW (2005) BK channel beta4 subunit reduces dentate gyrus excitability and protects against temporal lobe seizures. *Nat Neurosci* **8**:1752-1759.

Brenner R, Jegla TJ, Wickenden A, Liu Y and Aldrich RW (2000a) Cloning and functional characterization of novel large conductance calcium-activated potassium channel beta subunits, hKCNMB3 and hKCNMB4. *J Biol Chem* **275**:6453-6461.

Brenner R, Perez GJ, Bonev AD, Eckman DM, Kosek JC, Wiler SW, Patterson AJ, Nelson MT and Aldrich RW (2000b) Vasoregulation by the beta1 subunit of the calcium-activated potassium channel. *Nature* **407**:870-876.

Doherty JB, Chen M-H, Liu L, Natarajan SR and Tynerbor RM. Ophthalmic compositions for treating ocular hypertension. US 2004/0097575 A1. 2004. Ref Type: Patent

Galvez A, Gimenez-Gallego G, Reuben JP, Roy-Contancin L, Feigenbaum P, Kaczorowski GJ and Garcia ML (1990) Purification and characterization of a unique, potent, peptidyl probe for the high conductance calcium-activated potassium channel from venom of the scorpion Buthus tamulus. *J Biol Chem* **265**:11083-11090.

Garcia-Calvo M, Knaus HG, McManus OB, Giangiacomo KM, Kaczorowski GJ and Garcia ML (1994) Purification and reconstitution of the high-conductance, calcium-activated potassium channel from tracheal smooth muscle. *J Biol Chem* **269**:676-682.

Garcia-Valdes J, Zamudio FZ, Toro L and Possani LD (2001) Slotoxin, alphaKTx1.11, a new scorpion peptide blocker of MaxiK channels that differentiates between alpha and alpha+beta (beta1 or beta4) complexes. *FEBS Lett* **505**:369-373.

Ghatta S, Lozinskaya I, Lin Z, Gordon E, Willette RN, Brooks DP and Xu X (2007) Acetic acid opens large-conductance Ca2+-activated K+ channels in guinea pig detrusor smooth muscle cells. *Eur J Pharmacol* **563**:203-208.

Ghatta S, Nimmagadda D, Xu X and O'Rourke ST (2006) Large-conductance, calcium-activated potassium channels: structural and functional implications. *Pharmacol Ther* **110**:103-116.

Giangiacomo KM, Garcia ML and McManus OB (1992) Mechanism of iberiotoxin block of the large-conductance calcium-activated potassium channel from bovine aortic smooth muscle. *Biochemistry* **31**:6719-6727.

Heppner TJ, Bonev AD and Nelson MT (1997) Ca(2+)-activated K+ channels regulate action potential repolarization in urinary bladder smooth muscle. *Am J Physiol* **273**:C110-C117.

Knaus HG, Garcia-Calvo M, Kaczorowski GJ and Garcia ML (1994a) Subunit composition of the high conductance calcium-activated potassium channel from smooth

muscle, a representative of the mSlo and slowpoke family of potassium channels. *J Biol Chem* **269**:3921-3924.

Knaus HG, McManus OB, Lee SH, Schmalhofer WA, Garcia-Calvo M, Helms LM, Sanchez M, Giangiacomo K, Reuben JP, Smith AB, III and . (1994b) Tremorgenic indole alkaloids potently inhibit smooth muscle high-conductance calcium-activated potassium channels. *Biochemistry* **33**:5819-5828.

Lippiat JD, Standen NB, Harrow ID, Phillips SC and Davies NW (2003) Properties of BK(Ca) channels formed by bicistronic expression of hSloalpha and beta1-4 subunits in HEK293 cells. *J Membr Biol* **192**:141-148.

McManus OB, Helms LM, Pallanck L, Ganetzky B, Swanson R and Leonard RJ (1995) Functional role of the beta subunit of high conductance calcium-activated potassium channels. *Neuron* **14**:645-650.

Meera P, Wallner M and Toro L (2000) A neuronal beta subunit (KCNMB4) makes the large conductance, voltage- and Ca2+-activated K+ channel resistant to charybdotoxin and iberiotoxin. *Proc Natl Acad Sci U S A* **97**:5562-5567.

Miller C, Moczydlowski E, Latorre R and Phillips M (1985) Charybdotoxin, a protein inhibitor of single Ca2+-activated K+ channels from mammalian skeletal muscle. *Nature* **313**:316-318.

Rials SJ, Wu Y, Xu X, Filart RA, Marinchak RA and Kowey PR (1997) Regression of left ventricular hypertrophy with captopril restores normal ventricular action potential

duration, dispersion of refractoriness, and vulnerability to inducible ventricular fibrillation. *Circulation* **96**:1330-1336.

Sanchez M and McManus OB (1996) Paxilline inhibition of the alpha-subunit of the high-conductance calcium-activated potassium channel. *Neuropharmacology* **35**:963-968.

Shieh CC, Turner SC, Zhang XF, Milicic I, Parihar A, Jinkerson T, Wilkins J, Buckner SA and Gopalakrishnan M (2007) A-272651, a nonpeptidic blocker of large-conductance Ca(2+)-activated K(+) channels, modulates bladder smooth muscle contractility and neuronal action potentials. *Br J Pharmacol*.

Tammaro P, Smith AL, Hutchings SR and Smirnov SV (2004) Pharmacological evidence for a key role of voltage-gated K+ channels in the function of rat aortic smooth muscle cells. *Br J Pharmacol* **143**:303-317.

Wallner M, Meera P and Toro L (1999) Molecular basis of fast inactivation in voltage and Ca2+-activated K+ channels: a transmembrane beta-subunit homolog. *Proc Natl Acad Sci U S A* **96**:4137-4142.

Wang G and Lemos JR (1995) Tetrandrine: a new ligand to block voltage-dependent Ca2+ and Ca(+)-activated K+ channels. *Life Sci* **56**:295-306.

Wu SN, Li HF and Lo YC (2000) Characterization of tetrandrine-induced inhibition of large-conductance calcium-activated potassium channels in a human endothelial cell line (HUV-EC-C). *J Pharmacol Exp Ther* **292**:188-195.

Xia XM, Ding JP and Lingle CJ (2003) Inactivation of BK channels by the NH2 terminus of the beta2 auxiliary subunit: an essential role of a terminal peptide segment of three hydrophobic residues. *J Gen Physiol* **121**:125-148.

Xia XM, Ding JP, Zeng XH, Duan KL and Lingle CJ (2000) Rectification and rapid activation at low Ca2+ of Ca2+-activated, voltage-dependent BK currents: consequences of rapid inactivation by a novel beta subunit. *J Neurosci* **20**:4890-4903.

Xu CQ, Brone B, Wicher D, Bozkurt O, Lu WY, Huys I, Han YH, Tytgat J, Van Kerkhove E and Chi CW (2004) BmBKTx1, a novel Ca2+-activated K+ channel blocker purified from the Asian scorpion Buthus martensi Karsch. *J Biol Chem* **279**:34562-34569.

Yao J, Chen X, Li H, Zhou Y, Yao L, Wu G, Chen X, Zhang N, Zhou Z, Xu T, Wu H and Ding J (2005) BmP09, a "long chain" scorpion peptide blocker of BK channels. *J Biol Chem* **280**:14819-14828.

Zeng H, Lozinskaya IM, Lin Z, Willette RN, Brooks DP and Xu X (2006) Mallotoxin is a novel human ether-a-go-go-related gene (hERG) potassium channel activator. *J Pharmacol Exp Ther* **319**:957-962.

Footnotes

H.Z. and E.G. contributed equally to this study.

H.Z., current address: Merck Research Laboratories, West Point, PA 19486

JPET Fast Forward. Published on June 30, 2008 as DOI: 10.1124/jpet.108.139733
This article has not been copyedited and formatted. The final version may differ from this version.

Legends for figures

Figure 1. HMIMP blocked BK α subunit. (A) BK currents elicited from a CHO cell stably expressing BK α subunit using the voltage protocol shown in the inset before and after application of 30 nM HMIMP. (B) Concentration-responses of BK α subunit to HMIMP at voltage pulses of +80, +100, +120, and +140 mV were obtained as described in text (n=5). (C) From left to right: control BK currents, the first group and the twelfth group of BK currents induced after 5 min perfusion in 3 nM HMIMP without stimulation.

Figure 2. HMIMP blocks BK channels with different β subunits and BK channels from native tissues. BK $\alpha+\beta_1$ current (A, n=4~10) and BK $\alpha+\beta_4$ current (B, n=4) were elicited using the voltage protocol depicted in Fig. 1A inset. The corresponding concentration-responses were measured at the voltage step of +100 mV. Example BK current traces prior to and after 10 nM HMIMP application were shown as insets. HMIMP blocked BK channels in freshly isolated rabbit detrusor smooth muscle cells (C) and mouse vagal neuron (D). Inset: example BK current traces induced by depolarizing the cell (+10 to +80 mV in 10-mV increments) from a holding potential of 0 mV before and after 30 nM HMIMP. The current density and voltage relationship in control and 30 nM HMIMP was the average result of 16 detrusor and 3 neuron cells, respectively.

Figure 3. The effect of HMIMP on BK α single channel activity. Under symmetrical K^+ conditions, the inside-out patch was held at +80 mV and single channel activity was recorded for control and in HMIMP. (A) Open probability versus time histograms under control (left panel) and in the presence of 10 nM HMIMP (right panel). (B) Single

channel current traces obtained in control (left panel) and after exposure to 10 nM HMIMP (right panel), arrows indicate the zero current level. The regions highlighted are shown as insets below each trace to emphasize the single channel transitions on an expanded time scale. (C) Amplitude histograms from control (left panel) and after perfusion with 10 nM HMIMP (right panel). The amplitude histograms are not representative of the open probability of the entire trace. The open (D) and the close (E) time histograms in control (left panel) and after addition of 10 nM HMIMP (right panel).

Figure 4. HMIMP had no effect on Na^+ or Ca^{2+} channels. Human $Na_V1.5$ (A), $Ca_V3.2$ (B) or guinea pig ventricular myocyte L-type Ca^{2+} currents (C) were elicited with the corresponding voltage-clamp protocol (insets). Example current traces in control (top) and after HMIMP treatment (bottom) were shown on the left. The normalized I-V curves were shown on the right (n=4-6).

Figure 5. HMIMP had little effect on hERG channels. (A) hERG current was induced with the pulse protocol (inset) before and after 100 nM HMIMP treatment. The normalized I-V curve (B) and the voltage-dependent activation curve (C) of hERG channels in the absence and the presence of 100 nM HMIMP were generated as described in text. *, $P<0.05$, drug versus control.

Figure 6. HMIMP had no effect on cardiovascular potassium channels. Human KCNQ1+minK (A), rabbit ventricle I_{to} (B), or guinea pig arterial smooth muscle K_v currents (C) were elicited using the pulse protocols (insets). Example current traces in

control (top) and after HMIMP treatment (bottom) were shown on the left. The normalized I-V curve before (square) and after (circle) 100 nM HMIMP treatment were shown on the right (n=4-6).

Figure 7. HMIMP had no effect on ventricular action potentials but prolonged detrusor smooth muscle action potential. Action potentials recorded from a guinea pig ventricular myocyte (top), a rabbit ventricular myocyte (middle), and a guinea pig detrusor smooth muscle cell (bottom) before and after HMIMP treatment.

Figure 8. Comparing the chemical structure of HMIMP and Paxilline.

Fig. 1

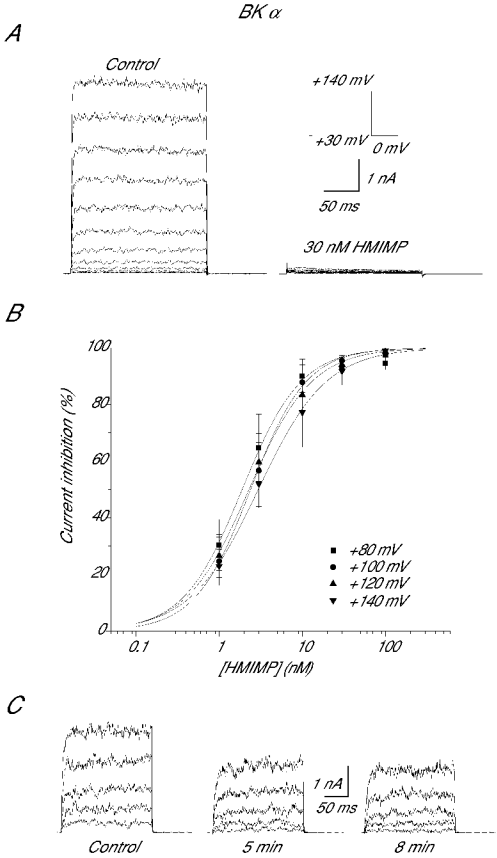
BK α
A
Control
+140 mV
+30 mV
0 mV
1 nA
50 ms
30 nM HMIMP
B
Current inhibition (%)
100
80
60
40
20
0
0.1
1
10
100
[HMIMP] (nM)
+80 mV
+100 mV
+120 mV
+140 mV
C
1 nA
50 ms
Control
5 min
8 min

Fig. 2

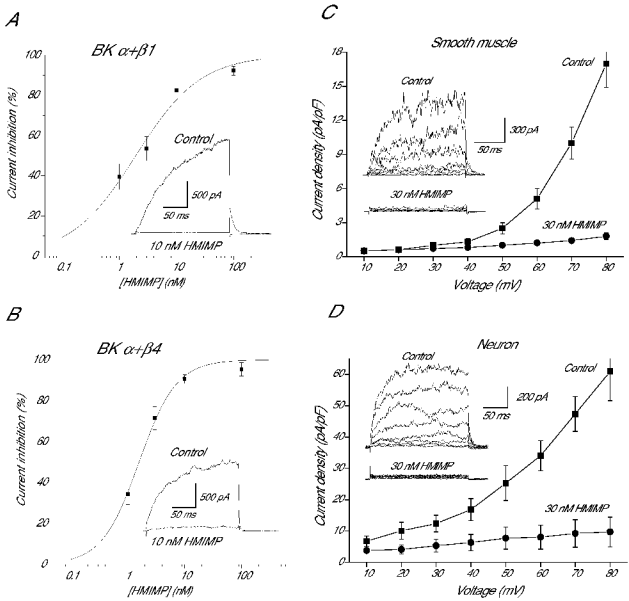
A
BK α+β1
Current inhibition (%)
[HMIMP] (nM)
Control
500 pA
50 ms
10 nM HMIMP
B
BK α+β4
Current inhibition (%)
[HMIMP] (nM)
Control
500 pA
50 ms
10 nM HMIMP
C
Smooth muscle
Current density (pA/pF)
Voltage (mV)
Control
300 pA
50 ms
30 nM HMIMP
30 nM HMIMP
D
Neuron
Current density (pA/pF)
Voltage (mV)
Control
200 pA
50 ms
30 nM HMIMP
30 nM HMIMP

Fig. 3

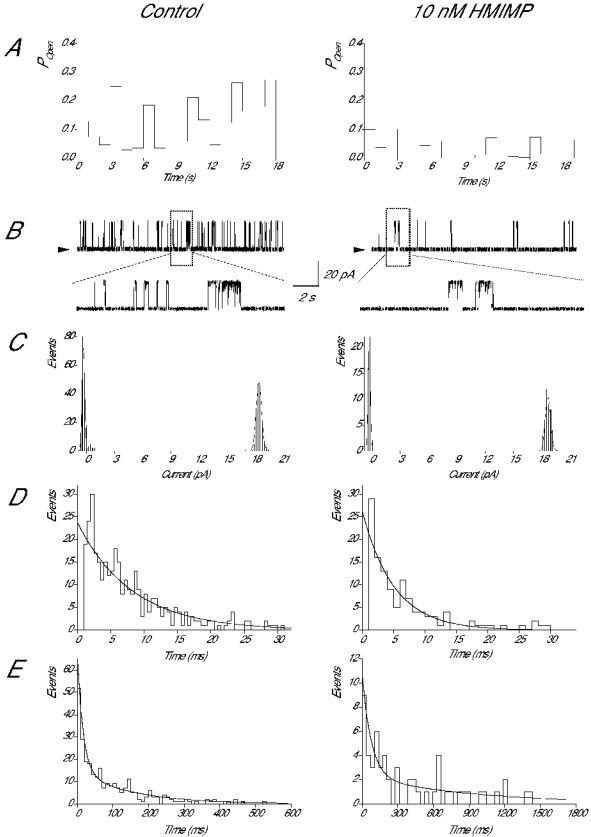
Control
10 nM HMIMP
A
B
C
D
E
Time (s)
20 pA
2 s
Events
Current (pA)
Time (ms)

Fig. 4

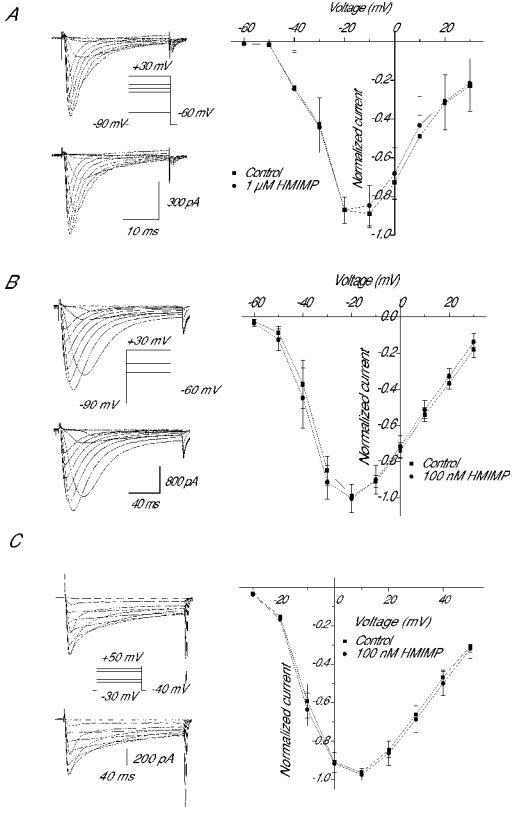
A
+30 mV
-90 mV
-60 mV
300 pA
10 ms
Voltage (mV)
-80
-40
-20
0
20
-0.2
-0.4
-0.6
-0.8
-1.0
Normalized current
Control
1 μM HMIMP
B
+30 mV
-90 mV
-60 mV
800 pA
40 ms
Voltage (mV)
-60
-40
-20
0
20
0.0
-0.2
-0.4
-0.6
-0.8
-1.0
Normalized current
Control
100 nM HMIMP
C
+50 mV
-30 mV
-40 mV
200 pA
40 ms
20
0
20
40
-0.2
-0.4
-0.6
-0.8
-1.0
Voltage (mV)
Control
100 nM HMIMP
Normalized current

Fig. 5

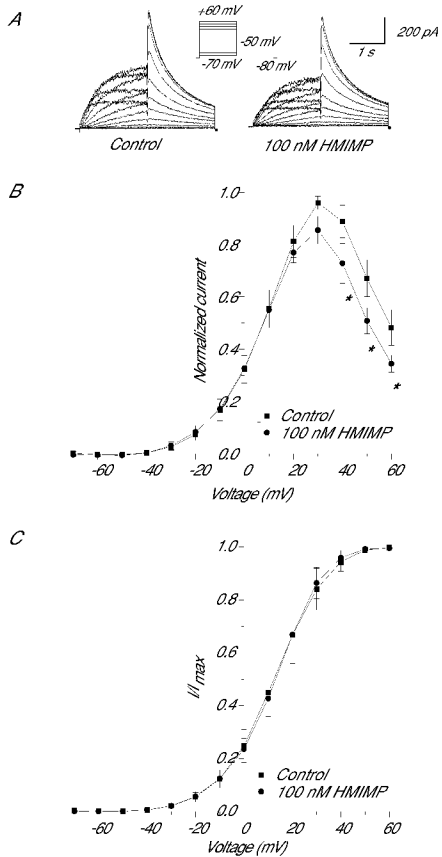
A
+60 mV
-50 mV
-70 mV
-80 mV
200 pA
1 s
Control
100 nM HMIMP
B
Normalized current
1.0
0.8
0.6
0.4
0.2
0.0
-60
-40
-20
0
20
40
60
Voltage (mV)
Control
100 nM HMIMP
C
I/I max
1.0
0.8
0.6
0.4
0.2
0.0
-60
-40
-20
0
20
40
60
Voltage (mV)
Control
100 nM HMIMP

Fig. 6

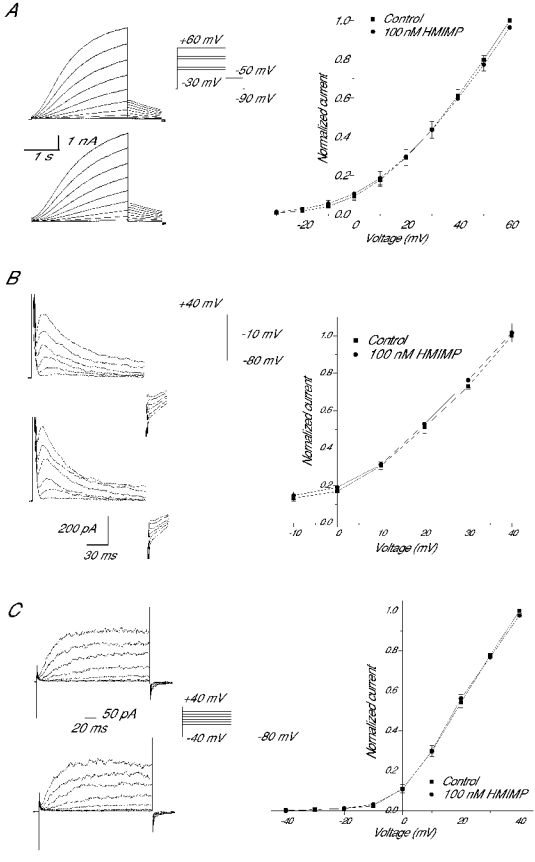
A
+60 mV
-50 mV
-30 mV
-90 mV
1 nA
1 s
Control
100 nM HMIMP
Normalized current
Voltage (mV)
B
+40 mV
-10 mV
-80 mV
200 pA
30 ms
Control
100 nM HMIMP
Normalized current
Voltage (mV)
C
50 pA
20 ms
+40 mV
-40 mV
-80 mV
Control
100 nM HMIMP
Normalized current
Voltage (mV)

Fig. 7

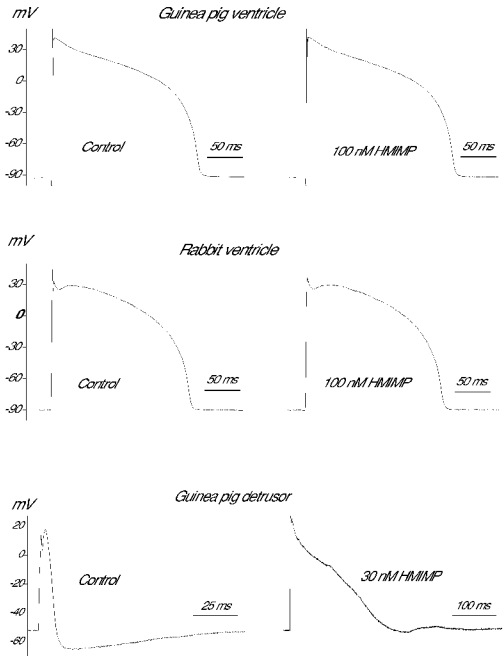
mV
Guinea pig ventricle
30
0
-30
-60
-90
Control
50 ms
100 nM HMMP
50 ms
mV
Rabbit ventricle
30
0
-30
-60
-90
Control
50 ms
100 nM HMMP
50 ms
mV
Guinea pig detrusor
20
0
-20
-40
-60
Control
25 ms
30 nM HMMP
100 ms

Fig. 8

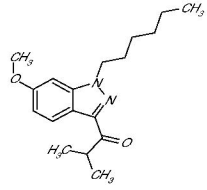

HMIMP

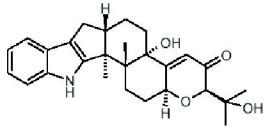

Paxilline